*Korean J. Chem. Eng.*, 32(9), 1889-1895 (2015)
DOI: 10.1007/s11814-014-0395-6

pISSN: 0256-1115
eISSN: 1975-7220

# Combined adsorption and reduction of Cr(VI) from aqueous solution on polyaniline/multiwalled carbon nanotubes composite

**Jiahong Wang*,**,†, Xiaolong Yin*, Wei Tang**, and Hongrui Ma*,****

*College of Resource and Environment, Shannxi University of Science & Technology, Xi'an 710021, China
**Shaanxi Research Institute of Agricultural Products Processing Technology, Xi'an 710021, China
(*Received 3 November 2014 • accepted 30 December 2014*)

**Abstract**−Polyaniline/multiwalled carbon nanotube (PANI-MWCNT) was prepared by bounding polyaniline on the surface of oxidized multiwalled carbon nanotube. The structure and surface properties of synthesized composites were characterized by Fourier transformed infrared spectroscopy (FTIR), X-ray photoelectron spectroscopy (XPS), X-ray diffraction (XRD), transmission electron microscope (TEM), and its adsorption capability for aqueous Cr(VI) was also studied. Characterized results showed that polyaniline was successfully anchored on the surface of MWCNT. From adsorption experiments the maximum adsorption amount of Cr(VI) onto PANI-MWCNTs was 28.25, 31.75 and 36.76 $mg \cdot g^{-1}$ at 15, 25 and 35 °C. Thermodynamic parameters showed that the Cr(VI) adsorption process was endothermic, spontaneous and feasible. Cr(VI) adsorption followed pseudo-second-order kinetics. Cr(VI) adsorption on the adsorbent decreases with increasing solution pH. The presence of anions in solution almost has no effect on Cr(VI) adsorption, indicating good selectivity. XPS analysis confirms that electrostatic interaction, reduction and chelation contribute to enhanced Cr(VI) removal. Cr(VI) loaded absorbent can be readily desorbed in 0.1 $mol \cdot L^{-1}$ of NaOH solution, and the desorption rate was 84.12%.

Keywords: Polyaniline/Multiwalled Carbon Nanotube, Hexavalent Chromium, Adsorption, Desorption

## INTRODUCTION

Wastewater containing chromium is commonly present in electroplating, electronics, metallurgy, leather tanning, textile and various other industry production [1], which poses severe threats to public health. Hexavalent chromium (Cr(VI)) is known to be highly toxic and carcinogenic. Various approaches, such as chemical reduction, precipitation, ion exchange, membrane separation, electrolytic reduction, adsorption and so on, have been developed to remove Cr(VI) from wastewater [2-5]. Due to its simplicity and high efficiency, adsorption has been considered as an effective method for the removal of Cr(VI) [6,7], and the success of adsorption technique depends on development of suitable adsorbents.

Carbon nanotubes with large specific surface areas and small, hollow, layered structures have been considered as promising adsorbents for various heavy metals [8-10]. However, their negatively charged surface, insolubility and the agglomerate formation in aqueous solution limited their application for the removal of aqueous Cr(VI) [11]. Many studies, therefore, have focused on surface modification to improve their adsorption capacity [12-14]. As Cr(VI) exists in water as oxyanions, amino adsorbents with positively charged nitrogen-containing functional groups have been found to be effective for the removal of Cr(VI). Polyaniline with advantages of easy synthesis, low cost, excellent environmental stability and large amount of amino and imine nitrogen groups have been frequently used as an efficient adsorbent for the removal of aqueous Cr(VI). For example, polyaniline [15], polypyrrole-polyaniline nanofiber [16], poly (aniline-1, 8-diaminonaphthalene) [17], polyaniline coated ethyl cellulose [18], polyaniline-magnetic mesoporous silica composite [19], polyaniline/bacterial extracellular polysaccharide nanocomposite [20] and polyaniline/montmorillonite composite [21], have been found to exhibit high adsorption affinity for aqueous Cr(VI). Therefore, coating polyaniline on the surface of MWCNT may enhance Cr(VI) adsorption. However, to our best knowledge, few studies have been conducted on the adsorption properties of polyaniline/carbon nanotubes composites for the removal of aqueous Cr(VI).

In this study, polyaniline/multiwalled carbon nanotubes composite (PANI-MWCNT) was prepared and applied to remove aqueous Cr(VI) from aqueous solution. Adsorption and desorption behavior of Cr(VI) on PANI-MWCNT was conducted by batch experiments. The effect of solution pH and ionic strength was also studied. The possible adsorption mechanism was advised based on adsorption experiment and XPS analysis.

## MATERIALS AND METHODS

### 1. Chemical Reagents

Multiwalled carbon nanotube (MWCNT) was purchased from Shenzhen carbon nanotech port Co., Ltd. The surface area was 100-120 $m^2 \cdot g^{-1}$, length was below 2 μm, and the diameter was 10-20 nm. Potassium dichromate of spectrophotometric purity and other reagents of analytical grade were supplied by Sinopharm Chemical reagent Co., Ltd.

†To whom correspondence should be addressed.
E-mail: wangjiahong@sust.edu.cn

**2. Preparation and Characterization of PANI-MWCNTs**

PANI-MWCNT was synthesized by two steps. First, MWCNT was pretreated by mixed acid. In detail, 1 g MWCNT was added to the flasks containing 240 ml of mixed acid (the volume ratio of concentrated sulfuric acid and concentrated nitric acid is 3 : 1). After being sonicated for 6 h at 60 °C, the mixed acid was filtered by 0.45 μm acid membrane, and the solid was washed with deionized water until neutral, followed by drying at 80 °C under vacuum. The resulting solid was referred to as O-MWCNT.

One milligram O-MWCNT and 0.4 ml of aniline were dispensed in a flask receiving 200 ml 1 mol·L$^{-1}$ HCl solution and sonicated for 30 min under $N_2$ (80 ml·min$^{-1}$) at room temperature. Then the suspension was stirred for 20 min in ice water. Ammonium persulfate solution (1.08 g of ammonium persulfate was dissolved in 80 ml 1 mol·L$^{-1}$ HCl) was pre-cooled to 0-4 °C and dropwise added to the above mixture. After stirring for 6 h, 40 ml acetone was added to terminate the polymerization reaction. The resulting solids were centrifuged and thoroughly washed several times with deionized water until colorless and neutral, followed by drying at 60 °C under vacuum for 24 h.

**3. Adsorbent Characterization**

Structural properties of the adsorbent surface were characterized by chemical analysis. Infrared spectra were recorded on a Vector-22 FTIR spectrometer (Germany) with the KBr pellet technology. XPS (Kratos AXIS Ultra DLD, England) equipped with a monochromatized AlKa X-ray radiation at 1486.6 ev was used to analyze the surface properties of the samples. The X-ray diffraction (XRD) patterns were recorded on an X-ray diffractometer (Japan). TEM observations were collected on a TEM-3010 transmission electron microscope (Japan).

**4. Batch Adsorption Experiment**

PANI-MWCNT was used as an adsorbent to study the adsorption behavior of Cr(VI) in aqueous solution. The equilibrium adsorption time was 24 h, and solution pH was adjusted with 0.1 mol·L$^{-1}$ NaOH or 0.1 mol·L$^{-1}$ HCl. The concentration of Cr(VI) was measured at 540 nm with diphenylcarbazide hydrazine spectrophotometry.

Adsorption isotherms at 15, 25 and 35 °C were conducted as follows: 20 mg PANI-MWCNT was added to glass tubes receiving 40 ml of Cr(VI) with initial Cr(VI) concentration from 20 to 100 mg·L$^{-1}$ at pH 4.5. The mixture was placed in a thermostatic shaker operated at 15, 25 and 35 °C, respectively. After achieving adsorption euquilibrium, the solutions were filtered and the residual concentrations of Cr(VI) were measured. The adsorption amounts of Cr(VI) on PANI-MWCNT were calculated according to Eq. (1):

$$q_e = \frac{(C_o - C_e) \times V}{m} \quad (1)$$

where $q_e$ (mg·g$^{-1}$) is the amount of Cr(VI) adsorbed at equilibrium, $C_o$ is the initial concentration of Cr(VI) (mg·L$^{-1}$), $C_e$ is the equilibrium Cr(VI) concentration (mg·L$^{-1}$), V is the volume of Cr(VI) solution (L), and m is the adsorbent mass (g).

Briefly, 200 mg PANI-MWCNT was dispensed in 500 ml three necks flask, receiving 500 ml Cr(VI) with initial concentration of 10, 20, and 40 mg·L$^{-1}$ at pH 4.5, respectively, and the mixture was stirred at 25 °C. A certain amount of the mixture was withdrawn and filtered for the determination of residual Cr(VI) concentration at different time intervals. Then the adsorption amounts of Cr(VI) on PANI-MWCNT were calculated according to Eq. (1).

The effect of solution pH on Cr(VI) adsorption was studied by dispensing 20 mg PANI-MWCNT in 40 ml of 40 mg·L$^{-1}$ Cr(VI) solution, and the pH values were adjusted from approximately 2 to 10 with 0.1 mol·L$^{-1}$ HCl or NaOH solution; the mixture was then placed in a thermostatic shaker operated at 25 °C. After 24 h adsorption, the solutions were filtered and the adsorption amounts of Cr(VI) on PANI-MWCNTs were calculated according to Eq. (1). The effect of co-existing anions was conducted with anionic concentration ($Cl^-$, $NO_3^-$, $SO_4^{2-}$) of 10 mmol·L$^{-1}$ at pH 4.5.

**5. Desorption**

Desorption kinetics was conducted in alkaline solution. In detail, 50 mg PANI-MWCNT was added to 100 ml of 100 mg·L$^{-1}$ Cr(VI) solution, and the mixture was placed in a thermostatic shaker operated at 25 °C for 24 h. After reaching adsorption equilibrium, the mixture was centrifuged and measured for determination of Cr(VI) adsorbed. Then the Cr(VI) loaded adsorbent was dispersed in 200 ml 0.1 mol·L$^{-1}$ NaOH solution and stirred at 25 °C. A certain amount of the mixture was withdrawn and filtered for the determination of residual Cr(VI) concentration at different time intervals.

## RESULTS AND DISCUSSION

**1. Adsorbent Characterization**

The infrared spectra are shown in Fig. 1. For the O-MWCNT, the peaks at 3,424, 1,633, 1,396 and 1,120 cm$^{-1}$ are assigned to the vibration of -OH, -COOH, C=O band and C-O band, respectively [22,23]. For the PANI-MWCNT, the peaks at 1,585, 1,498, 1,309, and 1,157 cm$^{-1}$ are ascribed to the vibration of quinone ring, benzene ring, C-N band, and the vibration of the -N=Q=N- band. The peak at 839 cm$^{-1}$ is attributed to the bending vibration of the benzene ring. These peaks are the typical peaks of polyaniline, indicating of the successful coating of the polyaniline on O-MWCT. From Fig. 2, three elements (C1s, O1s and N1s) were observed from the

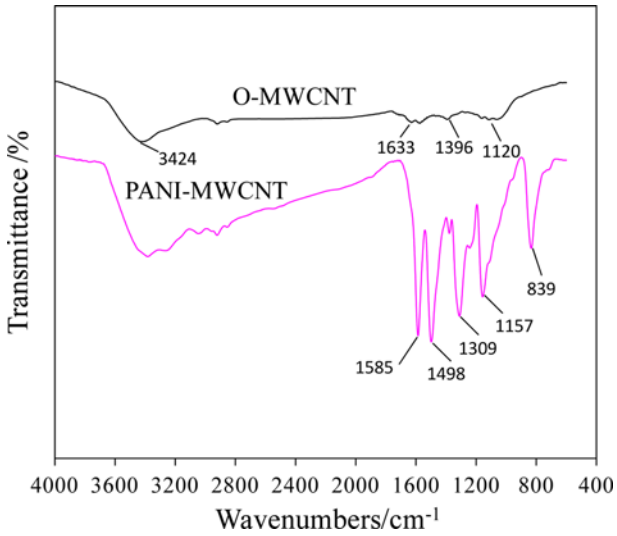


**Fig. 1. FTIR spectra of O-MWCNT and PANI-MWCNT.**

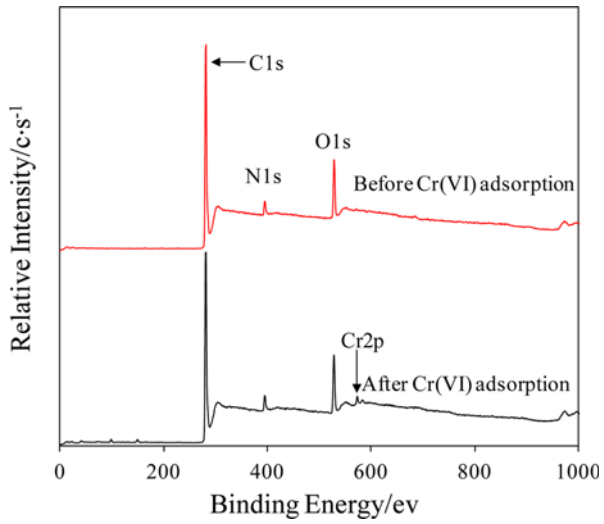


**Fig. 2. XPS survey spectrum of PANI-MWCNT before and after Cr(VI) adsorption.**

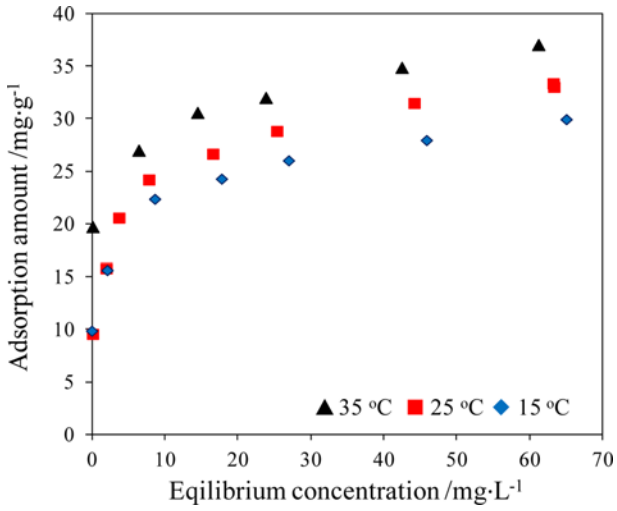


**Fig. 5. Adsorption isotherm of Cr(VI) on PANI-MWCNT at 15, 25 and 35 °C.**

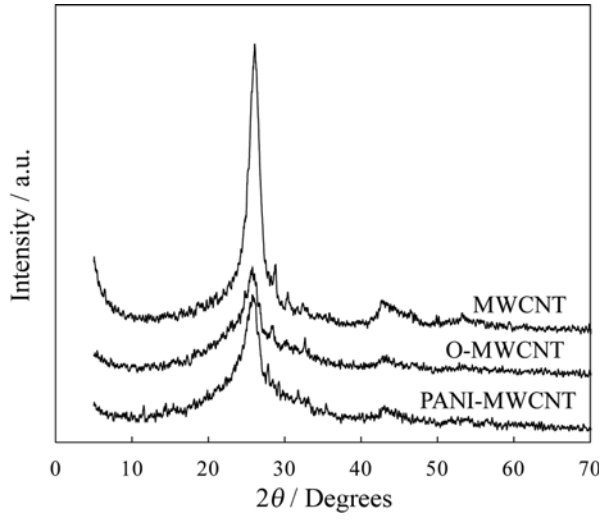


**Fig. 3. XRD patterns of the MWCNT, O-MWCNT, and PANI-MWCNT.**

XPS spectrum of PANI-MWCNT and the atom ratio was C, 87.73%; O, 8.77%; N, 3.51%.

The XRD patterns of the MWCNT, O-MWCNT, and PANI-MWCNT are shown in Fig. 3. For the MWCNT, a strong diffraction peak and a weak diffraction peaks with $2\theta$ at 26.6° and at 42.6° were observed, which corresponded to MWCNT and Ni(111) [24]. The same set of characteristic peaks was also appeared for O-MWCNT and PANI-MWCNT, which suggested that the crystal structure of O-MWCNT and PANI-MWCNT was well maintained. The reduced intensity of the characteristic peaks reflected that the polymer was coated on the surface of MWCNT.

TEM images of MWCNT and PANI-MWCT are shown in Fig. 4. From Fig. 4(a), the typical long tube of MWCNT was observed. From Fig. 4(b) and Fig. 4(c), after the polymerization reaction of aniline on the surface of MWCNT, the surface of MWCNT was encapsulated by shallow PANI layer. From Fig. 4(c), the end orifice of PANI-MWCNT was fully opened, which may be beneficial for the removal of aqueous Cr(VI). The BET surface area of PANI-MWCNT was 25.58 $m^2/g$.

**2. Adsorption Isotherms**

Adsorption isotherm is an important factor to explain the adsorption mechanism between adsorbent and adsorbate. Adsorption isotherms of Cr(VI) onto PANI-MWCNT at 15, 25 and 35 °C are shown in Fig. 5. From the result, the adsorption of Cr(VI) onto

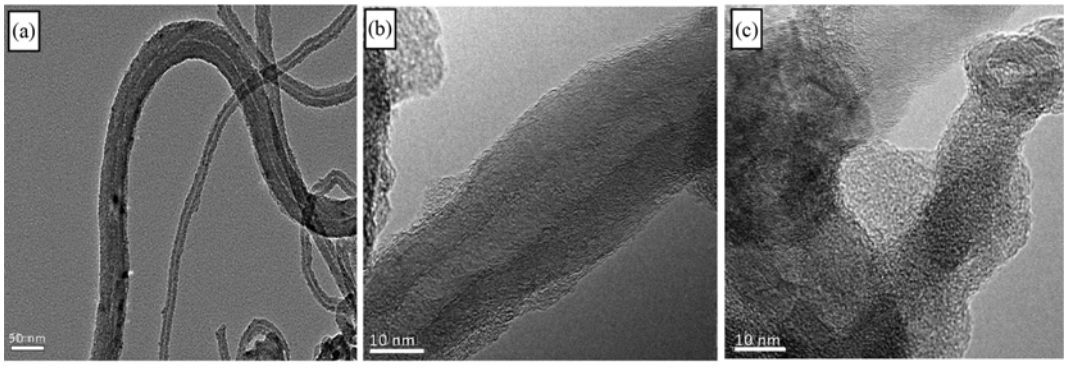


**Fig. 4. TEM of (a) MWCNT and (b), (c) PANI-MWCNT.**

PANI-MWCNT increased with the increasing of equilibrium Cr(VI) concentration. To further understand the adsorption mechanism, Langmuir and Freundlich equations were used to fit the experimental results [25].

Langmuir equation:

$$q_e = \frac{q_m b C_e}{1 + b C_e} \quad (2)$$

Freundlich equation:

$$q_e = K_f C_e^{1/n} \quad (3)$$

where $q_e$ (mg·g$^{-1}$) is the equilibrium adsorption amount, $q_m$ (mg·g$^{-1}$) is the theoretical adsorption capacity of adsorbent for Cr(VI), $C_e$ (mg·L$^{-1}$) is the equilibrium concentration of Cr(VI), b is the affinity coefficient (L·mg$^{-1}$). $K_f$ is Freundlich adsorption constant (L·mg$^{-1}$) and n is the characteristic constant associated with the temperature.

The parameters were calculated and tabulated in Table 1. From the results, the correlation coefficients ($R^2$) obtained from Freundlich equation are higher than Langmuir equation, indicating that the experimental data could be well described by Freundlich model. The results reflect that Cr(VI) adsorption on PANI-MWCNT tends to be a heterogeneous and multilayer adsorption process. Based on Langmuir adsorption process, the theoretical adsorption capacity at 15, 25 and 35 °C is 31.75 mg·g$^{-1}$, which is comparable with other carbon nanotube-based materials for Cr(VI) adsorption in aqueous solution (See in Table 2). The values of n are more than unity at all tested temperature, which confirms the favorable adsorption of Cr(VI) on the adsorbent.

To investigate the effect of temperature on the adsorption process, thermodynamic parameters such as the change in standard free energy $\Delta G^0$, enthalpy $\Delta H^0$, and entropy $\Delta S^0$ for Cr(VI) on PANI-MWCNT can be obtained from adsorption isotherms from the following equations:

$$\Delta G^0 = -RT \ln K_c \quad (4)$$

**Table 1. Langmuir and Freundlich model parameters for Cr(VI) adsorption on PANI-MWCNT at 15, 25 and 35 °C**

| Temperature (°C) | Freundlich model | | | Langmuir model | | |
|---|---|---|---|---|---|---|
| | $K_f$ | n | $R^2$ | $q_m$ | b | $R^2$ |
| 15 | 14.45 | 4.70 | 0.984 | 28.25 | 0.56 | 0.967 |
| 25 | 15.49 | 6.50 | 0.984 | 31.75 | 0.48 | 0.983 |
| 35 | 23.30 | 9.56 | 0.984 | 36.76 | 0.41 | 0.929 |

**Table 2. Maximum adsorption capacity of carbon nanotubes based adsorbents used for the removal of aqueous Cr(VI)**

| Adsorbent | Adsorption capacity (mg·g$^{-1}$) | pH | Reference |
|---|---|---|---|
| Carbon nanotube | 2.52 | 9.0 | [11] |
| Oxidized MWCNT | 4.26 | 2.05 | [12] |
| DP/MWCNTs | 55.555 | 2.0 | [14] |
| Activated carbon/CNTs | 9.0 | 2.0 | [26] |
| $CeO_2$/ACNTs | 30.2 | 7.0 | [27] |
| PANI-MWCNTs | 31.75 | 4.5 | Present study |

$$K_c = \frac{C_{Ae}}{C_{Se}} \quad (5)$$

$$\ln K_c = -\frac{\Delta H^0}{RT} + \frac{\Delta S^0}{R} \quad (6)$$

where $K_c$ is the equilibrium constant, R is the gas constant, T is the adsorption temperature, and $C_{Ae}$, $C_{Se}$ are the equilibrium concentration of Cr(VI) adsorbed on the adsorbents and in the solution, respectively.

The calculated thermodynamic parameters for Cr(VI) adsorption on PANI-MWCNT are tabulated in Table 3. From the results, the free energy value of $\Delta G^0$ is negative at all tested temperature and more negative at higher temperature, which indicates that Cr(VI) adsorption on PANI-MWCNT is spontaneous, and the spontaneity of adsorption process increases with temperature. The positive values of $\Delta H^0$ indicate that Cr(VI) adsorption on PANI-MWCNT is endothermic. In addition, the positive values of $\Delta S^0$ indicate that Cr(VI) adsorption on the adsorbent is an entropy-increasing process by the replacement of solvent molecules on adsorbent surface by sorbate molecules.

## 3. Adsorption Kinetics

Adsorption kinetics of Cr(VI) adsorption onto PANI-MWCNT at initial Cr(VI) concentration of 20, 40, and 80 mg·L$^{-1}$, respectively, and 25 °C is illustrated in Fig. 6. Cr(VI) adsorption amount on the adsorbent increased significantly in the beginning of adsorp-

**Table 3. Thermodynamic parameters of Cr(VI) adsorption on PANI-MWCNT**

| Cr(VI) concentration (mg/L) | $\Delta H^0$ (kJ/mol) | $\Delta S^0$ (J/(mol·K)) | $\Delta G^0$ (kJ/mol) | | |
|---|---|---|---|---|---|
| | | | 288 K | 298 K | 308 K |
| 20 | 17.81 | 126.90 | −18.81 | −19.90 | −21.35 |
| 40 | 12.16 | 99.30 | −16.45 | −17.43 | −18.44 |
| 60 | 10.97 | 91.40 | −15.35 | −16.28 | −17.18 |
| 80 | 10.08 | 86.00 | −14.68 | −15.53 | −16.40 |

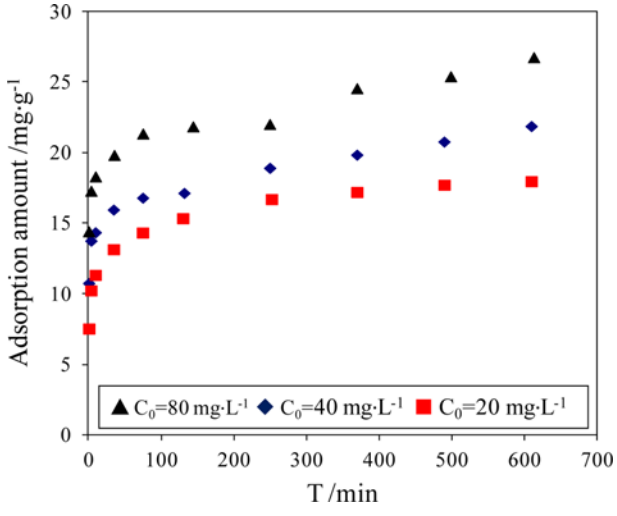


**Fig. 6. Adsorption kinetics of Cr(VI) adsorption onto PANI-MWCNT at initial Cr(VI) concentration of 20, 40 and 80 mg·L$^{-1}$, respectively, and 25 °C.**

**Table 4. Fitting parameters of Cr(VI) adsorption onto PANI-MWCNT using pseudo-first-order and pseudo-second-order kinetic models**

| $C_0$/mg·L$^{-1}$ | $q_{exp}$/mg·g$^{-1}$ | Pseudo-first-order kinetics | | | Pseudo-second-order kinetics | | |
|---|---|---|---|---|---|---|---|
| | | $k_1$/min$^{-1}$ | $q_{cal}$/mg·g$^{-1}$ | $R^2$ | $k_2$/g·mg$^{-1}$·min$^{-1}$ | $q_{cal}$/mg·g$^{-1}$ | $R^2$ |
| 20 | 24.24 | $4.15\times10^{-3}$ | 8.80 | 0.874 | $2.60\times10^{-3}$ | 19.19 | 0.996 |
| 40 | 27.25 | $3.92\times10^{-3}$ | 10.61 | 0.938 | $1.67\times10^{-3}$ | 23.20 | 0.995 |
| 80 | 33.39 | $3.45\times10^{-3}$ | 10.49 | 0.941 | $1.89\times10^{-3}$ | 27.25 | 0.994 |

tion process and gradually became stable with further extension of time. Pseudo-first-order and pseudo-second-order adsorption rate equations are widely used to simulate the adsorption data [28,29], which can be expressed as follows:

The pseudo-first-order adsorption equation:

$$\lg(q_e - q_t) = \lg q_e - \frac{k_1}{2.303}t \quad (7)$$

The pseudo-second-order adsorption equation:

$$\frac{t}{q_t} = \frac{1}{k_2 q_e^2} + \frac{1}{q_e}t \quad (8)$$

where $q_e$ (mg·g$^{-1}$) is the adsorption amount, $q_t$ (mg·g$^{-1}$) is the adsorption amount at time, $k_1$ (1/min) is the rate constant of pseudo-first-order adsorption, $k_2$ (g·mg$^{-1}$·min$^{-1}$) is the rate constant of pseudo-second-order adsorption.

Simulated parameters based on the pseudo-first-order and pseudo-second-order adsorption rate equation are given in Table 3. The correlation coefficient ($R^2$) for pseudo-second-order adsorption rate equation is higher than pseudo-first-order adsorption rate equation ($R^2$>0.99). The calculated equilibrium adsorption capacity is almost identical to the experiment data, which suggests that Cr(VI) adsorption onto PANI-MWCNT can be fitted by pseudo-second-order adsorption rate equation, indicative of chemical adsorption.

**4. Effect of Solution pH and Coexisted Anions on Cr(VI) Adsorption**

Effect of solution pH on Cr(VI) adsorption onto PANI-MWCNT is shown in Fig. 7. From the results, Cr(VI) adsorption amount on PANI-MWCNT decreased monotonically with an increase of solution pH, and the maximum adsorption amount of Cr(VI) was 75.59 mg·g$^{-1}$ at pH 2.0. This may be attributed to the physicochemical properties of adsorbents and Cr(VI). Cr(VI) in aqueous solution mainly exists in anionic form, such as $HCrO_4^-$, $CrO_4^{2-}$, $Cr_2O_7^{2-}$ and so on [15]. PANI-MWCNT would be positively charged due to the deprotonation of amino groups of PANI on surface of the adsorbent, which may invoke the electrostatic attraction with anionic Cr(VI), leading to the enhanced Cr(VI) adsorption. With increasing solution pH, the adsorbent may be negatively charged because of the deprotonation of amino groups of PANI on the surface of the adsorbent, and the electrostatic repulsion between the adsorbent and Cr(VI) may result in the reduced Cr(VI) adsorption.

The anions $Cl^-$, $NO_3^-$, and $SO_4^{2-}$ are frequently present in natural water, which would compete with anionic Cr(VI) for active sites on the adsorbent, therefore affecting the Cr(VI) adsorption on the adsorbent. Effect of $Cl^-$, $NO_3^-$, and $SO_4^{2-}$ in aqueous solution is illustrated in Fig. 8. Based on the plots, no obvious effect of $Cl^-$, $NO_3^-$, $SO_4^{2-}$ on Cr(VI) adsorption was observed, which indicates that the adsorbent has good selectivity.

**5. Adsorption Mechanism**

From Fig. 2, after Cr(VI) adsorption on PANI-MWCNT, the characteristic peak of Cr elements appears, which indicates that Cr(VI) has been successfully adsorbed on the surface of the adsorbent. To further describe the Cr(VI) adsorption mechanism, high resolution XPS spectra of N1s and Cr 2p were conducted and (see Fig. 9). For the N1s core level spectra of PANI-MWCNT, it can be

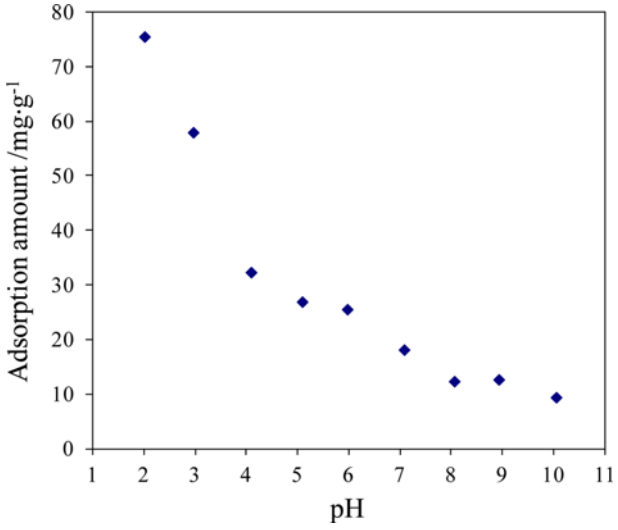


**Fig. 7. Effect of solution pH on Cr(VI) adsorption onto PANI-MWCNT.**

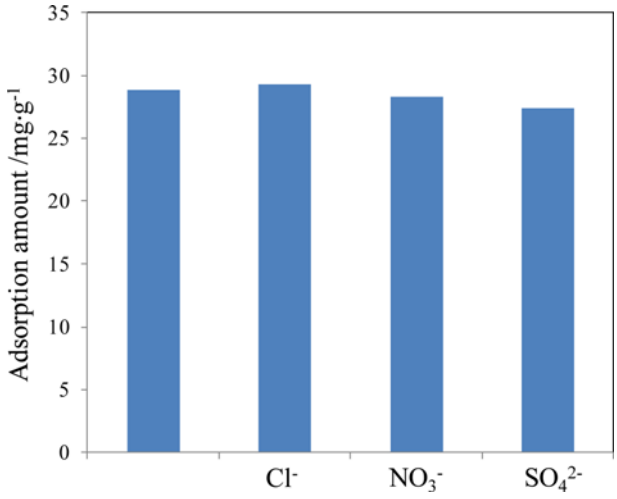


**Fig. 8. Effect of coexistence anion on Cr(VI) adsorption onto PANI-MWCNT.**

fitted into three peaks centered at binding energies of 398.6, 399.5, and 401.0 ev, which are assigned to the imine (-N=), amine (-NH-), and positively charged nitrogen (-$NH^{*+}$-), respectively. After Cr(VI) adsorption on the adsorbent, the similar three peaks were observed. However, the molar percent of -NH- decreased from 65.13% before Cr(VI) adsorption to 46.02% after Cr(VI) adsorption, and molar content of -$NH^{*+}$- increased from 14.68% before Cr(VI) adsorption to 25.50% after Cr(VI) adsorption, which demonstrates the doping adsorption of Cr(VI) during the adsorption. Meanwhile, the molar percent of -N= increased from 20.19% before Cr(VI) adsorption to 28.48% after Cr(VI) adsorption, which indicates the existence of redox reaction during Cr(VI) adsorption. This phenomenon can also be proved from the Cr 2p spectra in Fig. 9(b). From the results, 58.67% Cr(VI) adsorbed on PANI-MWCNT was reduced to Cr(III) [30]. Cr(III) adsorbed on the surface of adsorbent may be attributed to the chelation with nitrogen of PANI on the adsorbent [19].

## 6. Desorption

It can be inferred from the effect of pH that Cr(VI) saturated adsorbent can be desorbed in alkaline solution; therefore, 0.1 mol·$L^{-1}$ NaOH was used as a desorption agent. The desorption kinetic is shown in Fig. 10. From the result, the desorption rate increased with the increasing desorption time, and desorption equilibrium was achieved within 10 h. The maximum desorption rate of the loaded Cr(VI) absorbent was 84.12%, which indicates that Cr(VI) adsorbed on the adsorbent can be easily desorbed. This may be because the competitive adsorption of $OH^-$ with anionic Cr(VI) resulted in the desorption of Cr(VI).

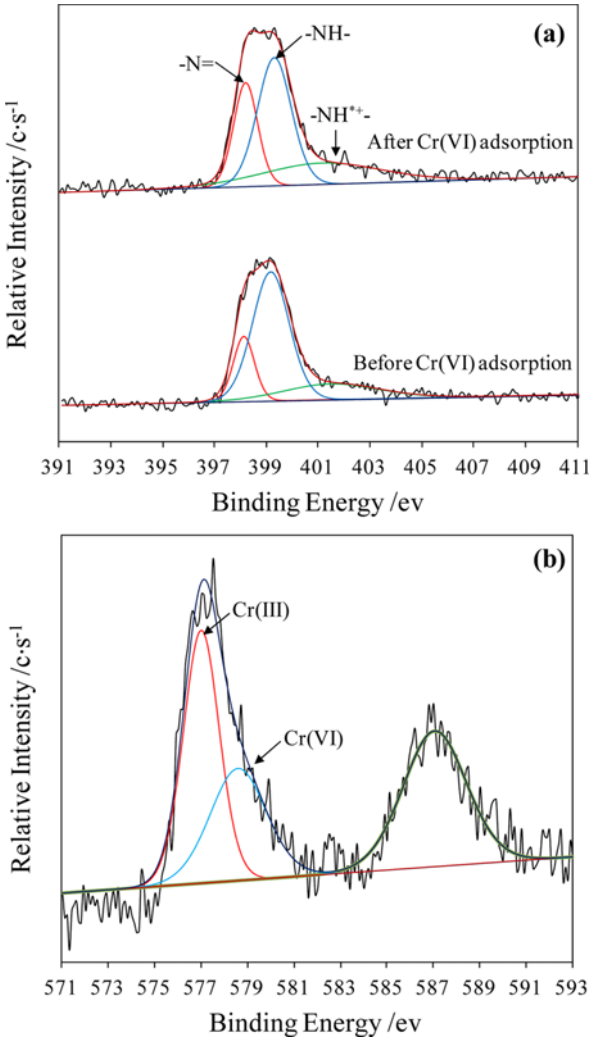


**Fig. 9. XPS N 1s (a) spectra of PANI-MWCNT before and after Cr (VI) adsorption, and Cr 2p (b) spectrum of PANI-MWCNT after Cr(VI) adsorption.**

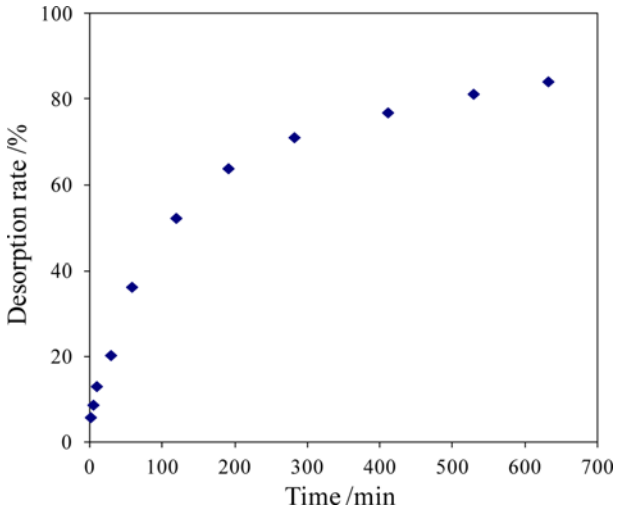


**Fig. 10. Desorption kinetic of Cr(VI) saturated PANI-MWCNT in 0.1 mol·$L^{-1}$ NaOH solution.**

## CONCLUSIONS

PANI-MWCNT composite was prepared by in situ polymerization on oxidized MWCNT and characterized by FITR, XPS, XRD, and TEM. Characterized results showed that PANI was successfully grafted on the surface of MWCNT. PANI-MWCNT has high adsorption affinity for aqueous Cr(VI), and adsorption isotherm could be fitted better by both Freundlich and Langmuir model, indicating heterogeneous monolayer adsorption. Cr(VI) adsorption onto PANI-MWCNT can be fitted by pseudo-second-order kinetics very well. Cr(VI) adsorption on the adsorbent decreased with an increase of solution pH and coexisting anions almost have no effluence on Cr(VI) adsorption. XPS analysis reveals that a mechanism of electrostatic attraction followed by reduction of Cr(VI) to Cr(III) and chelation adsorption was advised for Cr(VI) adsorption on PANI-MWCNT. Cr(VI) loaded absorbent can be readily desorbed in alkaline solution. The present results reflected that PANI-MWCNT can be used as a potential adsorbent for removing Cr(VI) from wastewater.

## ACKNOWLEDGEMENTS

This work was supported by National Science Foundation of China (21107065), Natural Science Basic Research Plan in Shaanxi Province (2012JQ2003), and Innovation Program of Scientific Research Group of Shaanxi Province (2014KCT-15), Xi'an and the State Key

Laboratory Program of Pollution Control and Resources Reuse (PCRRF11012), Nanjing China.

## REFERENCES


1. S. Zhang, M. Zeng, W. Xu, J. Li, J. Li, J. Xu and X. Wang, *Dalton T.*, **42**, 7854 (2013).
2. N. Meunier, P. Drogui, C. Montané, R. Hausler, G. Mercier and J. F. Blais, *J. Hazard. Mater.*, **137**, 581 (2006).
3. C. A. Kozlowski and W. Walkowiak, *Water Res.*, **36**, 4870 (2002).
4. L. A. M. Ruotolo, D. S. Santos-Júnior and J. C. Gubulin, *Water Res.*, **40**, 1555 (2006).
5. U. K. Garg, M. P. Kaur, V. K. Garg and D. Sud, *J. Hazard. Mater.*, **140**, 60 (2007).
6. H. I. Adegoke, F. AmooAdekola, O. S. Fatoki and B. J. Ximba, *Korean J. Chem. Eng.*, **31**, 142 (2014).
7. F. Gorzin and A. A. Ghoreyshi, *Korean J. Chem. Eng.*, **30**, 1594 (2013).
8. W. Konicki, I. Pelech and E. Mijowska, *Pol. J. Chem. Technol.*, **16**, 87 (2014).
9. D. K. V. Ramana, J. S. Yu and K. Seshaiah, *Chem. Eng. J.*, **223**, 806 (2013).
10. X. Y. Yu, T. Luo, Y. X. Zhang, Y. Jia, B. J. Zhu, X. C. Fu, J. H. Liu and X. J. Huang, *Acs Appl. Mater. Interf.*, **3**, 2585 (2011).
11. N. Mubarak, R. Thines, N. Sajuni, E. Abdullah, J. Sahu, P. Ganesan and N. Jayakumar, *Korean J. Chem. Eng.*, **31**, 1582 (2014).
12. J. Hu, C. Chen, X. Zhu and X. Wang, *J. Hazard. Mater.*, **162**, 1542 (2009).
13. X. Zhang, M. Chen, Y. Yu, T. Yang and J. Wang, *Anal. Methods*, **3**, 457 (2011).
14. R. Kumar, M. O. Ansari and M. A. Barakat, *Chem. Eng. J.*, **228**, 748 (2013).
15. K. K. Krishnani, S. Srinives, B. C. Mohapatra, V. M. Boddu, J. Hao, X. Meng and A. Mulchandani, *J. Hazard. Mater.*, **252-253**, 99 (2013).
16. M. Bhaumik, A. Maity, V. V. Srinivasu and M. S. Onyango, *Chem. Eng. J.*, **181-182**, 323 (2012).
17. Q. Li, Y. Qian, H. Cui, Q. Zhang, R. Tang and J. Zhai, *Chem. Eng. J.*, **173**, 715 (2011).
18. B. Qiu, C. Xu, D. Sun, H. Yi, J. Guo, X. Zhang, H. Qu, M. Guerrero, X. Wang, N. Noel, Z. Luo, Z. Guo and S. Wei, *ACS Sustain Chem. Eng.*, **2**, 2070 (2014).
19. L. Tang, Y. Fang, Y. Pang, G. M. Zeng, J. J. Wang, Y. Y. Zhou, Y. C. Deng, G. D. Yang, Y. Cai and J. Chen, *Chem. Eng. J.*, **254**, 302 (2014).
20. V. Janaki, M. N. Shin, S. H. Kim, K. J. Lee, M. Cho, A. K. Ramasamy, B. T. Oh and S. Kamala-Kannan, *Cellulose*, **21**, 463 (2014).
21. J. Chen, X. Hong, Y. Zhao and Q. Zhang, *Water Sci. Technol.*, **70**, 678 (2014).
22. S. Yang, J. Li, D. Shao, J. Hu and X. Wang, *J. Hazard Mater.*, **109**, 166 (2009).
23. M. Abdel Salam and R. C. Burk, *Appl. Surf. Sci.*, **255**, 1975 (2008).
24. W. Feng, W. Yi, Y. Xu, Y. Lian, X. Wang and Y. Katsumi, *Acta Phy. Sin.*, **52**, 1272 (2003).
25. J. Wang, Y. Ji, S. Ding, H. Ma and X. Han, *Chinese J. Chem. Eng.*, **21**, 594 (2013).
26. M. A. Atieh, *Procedia Environmental Sciences*, **4**, 281 (2011).
27. Z. C. Di, J. Ding, X. J. Peng, Y. H. Li, Z. K. Luan and J. Liang, *Chemosphere*, **62**, 861 (2006).
28. J. Wang, S. Ding, C. Zheng, H. Ma and Y. Ji, *Desalin. Water Treat.*, **40**, 92 (2012).
29. J. Wang, X. Han, H. Ma, Y. Ji and L. Bi, *Chem. Eng. J.*, **173**, 171 (2011).
30. W. Yu, L. Zhang, H. Wang and L. Chai, *J. Hazard. Mater.*, **260**, 789 (2013).